GEOLOGICA CARPATHICA, DECEMBER 2005, 56, 6, 493–502

Th-U-Pb dating of monazite from the Cretaceous uranium vein mineralization in the Permian rocks of the Western Carpathians

IGOR ROJKOVIČ[1] and PATRIK KONEČNÝ[2]

[1]Faculty of Natural Sciences, Comenius University, Mlynská dolina, 842 15 Bratislava, Slovak Republic; rojkovic@fns.uniba.sk
[2]Geological Survey of Slovak Republic, Mlynská dolina 1, 817 04 Bratislava, Slovak Republic; konecnyp@gssr.sk

(Manuscript received December 1, 2004; accepted in revised form June 16, 2005)

Abstract: Th-U-Pb dating of monazite confirms the Permian age 278 ± 11 Ma of rhyolite tuff in the Northern Gemericum. This rock was a protolith for stratiform U-Mo mineralization formed during the Late Permian by ground water. The Permian formations and stratiform mineralization are cut by younger vein and stockwork mineralization near Novoveská Huta and Krompachy. The quartz vein with uranium mineralization in Krompachy is accompanied by albite, rutile, sulphides, xenotime-(Y) and rare monazite-(Ce). Th-U-Pb dating of the vein monazite gives the Cretaceous age 124 ± 10 Ma of remobilized vein uranium mineralization.

Key words: Gemericum, age, vein mineralization, electron microprobe monazite dating, rhyolite tuff.

Introduction

Monazite, a REE phosphate commonly occurs in acid magmatic and metamorphic rocks. Occurrence of monazite in veins can explain hydrothermal processes. Hydrothermal vein mineralization in the Slovenské rudohorie Mts has long been discussed with regard to possible Hercynian and Alpine origin. The aim of this study was dating of monazite associated with uranium mineralization in this area.

The initial Th and U decay produce radiogenic Pb. On assumption that all Pb is only of radiogenic origin and the Th-U-Pb equilibrium was not disturbed by some geological event, the present concentration of Pb in the monazite is proportional to the age of radiogenic decay. The new generation of microprobes released in the last decade allows more precise measuring of low concentration of Pb in monazite. The first experience with monazite dating and formulation of the Th-U-Pb age calculations were brought by Parrish (1990), Suzuki & Adachi (1991, 1994), Suzuki et al. (1994) and Montel et al. (1996). Refinement of measurement conditions, correction of peak overlapping between Th-U-Pb-Y described in Suzuki & Adachi (1998), Fialin et al. (1999), Scherer et al. (2000), Pyle et al. (2002), Nagy (2003), Cocherie & Albarede (2001) led to overall improvement of monazite dating. The results of monazite dating can be found in a growing number of papers such as Cocherie et al. (1998), Suzuki & Adachi (1998), Finger & Broska (1999), Williams et al. (1999), Nagy et al. (2002), Finger et al. (2003), Kohn & Malloy (2004).

Geological setting

The Western Carpathians are divided from north to south into Outer, Central (CWC) and Inner Western Carpathians. The CWC consist of the following belts: Pieniny Klippen Belt, Tatra-Fatra Belt of core mountains, Vepor Belt and Gemer Belt in the south (Plašienka et al. 1997). The basement of the Gemericum sheet is composed of the Lower Paleozoic metasediments and metavolcanics cut by intrusions of small bodies of the Permian granites. This basement is structurally closely confined to Late Paleozoic volcano-sedimentary succession. The northern Gemeric Carboniferous rocks are represented by the Dobšiná Group (Vozárová & Vozár 1988).

The Krompachy Group represents the Permian rocks of the northern Gemeric Unit (Bajaník et al. 1981). The thickness of the Permian rocks near Novoveská Huta is variable up to 2.5 km (Novotný & Miháľ 1987). The sediments represent mesocycles of a continental character with the appearance of lagoonal lithofacies in the uppermost part. Three formations were distinguished (Bajaník et al. 1981):

1. the Knola Formation — coarse detritic sediments,
2. the Petrova Hora Formation — volcano-sedimentary rocks,
3. the Novoveská Huta Formation — fine clastic sediments with evaporites.

The sedimentary rocks of the Knola Formation are represented by red polymict conglomerate, sandstone and aleurolite formed in fanglomeratic, fluvial and limnic lithofacies (Rojkovič et al. 1993).

Volcano-sedimentary rocks of the Petrova Hora Formation are represented by polymict to monomict conglomerate, sandstone, aleurolite, tuffite, tuff and volcanics. Sedimentary and volcanic rocks were formed in the continental environment. Rhyolite, dacite and andesite are accompanied by volcanoclastics.

Andesite and dacite can be seen in the whole belt of the Permian rocks, but they are more abundant in area of Krompachy and Jahodná near Košice. The volcanic rocks are overlain by thick sequence of violet and green volcano-clastics forming carbonatized sericite-chlorite and quartz-sericite-chlorite shales. They are overlain by bombs and lapilli tuffs, especially in Krompachy area. Towards the south, epiclastics are more abundant and the rocks gain the character of tuffitic conglomerate (Rojkovič & Miháľ 1991).

Acid volcanic and volcanoclastic rocks overlying the andesite and dacite are abundant mainly in Petrova Hora. They are represented mostly by psammitic tuffs, ignimbrite and less by rhyolite. They are light green to light grey moderately schistose rocks. Fragments or phenocrysts are represented by quartz with magmatic corrosion, potassium feldspar, plagioclase, biotite and pseudomorphs of sericite after feldspars. Matrix with dominant quartz is microgranoblastic or lepidoblastic if sericite is more abundant. Ignimbrite shows typical textures with plastic deformation of glass fragments now recrystallized. Zircon and tourmaline are frequent, while monazite-(Ce), titanite and garnet are rare accessory minerals.

The uppermost formation of the Krompachy Group is the Novoveská Huta Formation, representing a complete sedimentary mesocycle. The sediments are finer upwards from basal polymict conglomerate through sandstone to shale with evaporite horizons containing carbonates, sulphates and halite. Sediments belong to fanglomerate-fluvial facies, limnic facies up to products of sea ingression with sulphates and halite.

All tectonic elements are Alpine, with prevalence of northern vergency, and they form a uniform fold and fault style of the regional structure (Rojkovič et al. 1993).

U-Mo mineralization is bound to the Petrova Hora Formation in the whole Permian belt in the northern Gemericum from Dobšiná in the west to Košice eastward. The most important uranium mineralization occurs near Novoveská Huta. Several occurrences of uranium mineralization of similar character as in Novoveská Huta occur near Krompachy and Petrova Hora. Important uranium deposit occurs in the eastern margin of this Permian belt near Košice. Uranium deposits form mostly stratiform (lenticular) and peneconcordant bodies in sandstones and conglomerates with volcanoclastic material and also directly in volcanic rocks.

The most important uranium mineralization in Novoveská Huta area occurs in two horizons of the Petrova Hora Formation. Ore bodies form lenses mostly concordant to wall rocks. Planes concordant to the Alpine cleavage are also locally mineralized. The length of the lower mineralized horizon is 4 km, the width varies from 200 to 600 m and the thickness reaches up to 80 meters. Lenticular ore bodies are several meters to tens of meters thick and their area extends from tens to tens of thousands of square meters. Intensive silicification, sericitization, carbonatization, pyritization and increased apatite and tourmaline contents characterize mineralized rocks. Uranium mineralization is disseminated or forms veinlets.

Uraninite and molybdenite are dominant in the U-Mo ores of both main horizons. They are accompanied by U-Ti oxides, pyrite, apatite, chalcopyrite, tennantite, galena, sphalerite, arsenopyrite, ilmenite, rutile, leucoxene, magnetite, hematite, covellite, marcasite, pyrrhotite, boulangerite, xenotime-(Y), monazite-(Ce), goethite, autunite and torbernite (Rojkovič 1968, 1997). Primary stratiform uranium mineralization was mostly formed at 100 to 150 °C according to the homogenization temperatures of fluid inclusions. Fluid concentration reached 27 to 33 equiv. wt. % NaCl. Remobilized U-Mo mineralization was formed at temperatures ranging from 320 to 240 °C with maximum at 250 °C. Fluid inclusions suggest the presence of Mg, K, Na, Cl in fluids and fluid concentration 10 to 15 equiv. wt. % NaCl. The *P-T* parameters of the Alpine metamorphic overprint of the Lower Paleozoic rocks of Gemericum were estimated to 330–350 °C and 0.5–0.6 GPa. The metamorphism of the Permian rocks was estimated to 270–300 °C and 0.3–0.4 GPa (Faryad & Dianiška 1999).

The stratiform uranium mineralization is cut by younger high-grade mineralization. High-grade uranium mineralization rarely occurs in faults and schistosity planes cutting the U-Mo mineralized horizons in the western part of the Novoveská Huta deposit. Mineralization has a disseminated, stockwork character containing fragments of the ore-bearing horizons in the faults. Fault-related ore 0.1 to 2 m thick is situated some hundreds of meters from its trans-section with the ore bearing horizons. Uranium and molybdenum mineralization is represented by uraninite, coffinite and molybdenite. Chalcopyrite, tennantite, pyrite, galena, U-Ti oxides, montroseite, marcasite, sphalerite, clausthalite, graphite, quartz and Fe-dolomite are accompanying minerals.

Uranium mineralization occurs southwest from Krompachy (Fig. 1), south of Jarček stream. Veinlets of quartz several centimeters thick cut green sandstone of the Novoveská Huta Formation. X-ray amorphous U-Ti oxides are abundant in quartz veinlets accompanied by albite, less by carbonate, columnar crystals of rutile, galena, pyrite, chalcopyrite, xenotime-(Y) and rare monazite-(Ce) (Rojkovič & Miháľ 1991). Mineralization is accompanied by red coloured alteration of sandstone due to hematite pigment.

Carbon and sulphur isotopic composition display the larger variabilities in stratiform U-Mo ores than in quartz-carbonate veins with Cu mineralization. $\delta^{34}S$ and $\delta^{13}C$ values vary in stratiform U-Mo ores from −32.7 to +2.7 ‰ and from −27.1 to −0.5 ‰, respectively. The wide range of the isotopic composition of C and S may be explained by mixing of ore forming fluids derived from sedimentary rocks with possible fluids of volcanic origin and by their complex history (metamorphism and remobilization) (Rojkovič 1997). $\delta^{13}C$ values around −21 ‰ propose a biogenic origin. Negative $\delta^{34}S$ values may suggest bacterial reduction or they are the result of partial isotopic equilibration of hydrogen sulphide of volcanic origin with sulphates derived from overlaying evaporites. The relatively narrower ranges of $\delta^{34}S$ and $\delta^{13}C$ values from −18.8

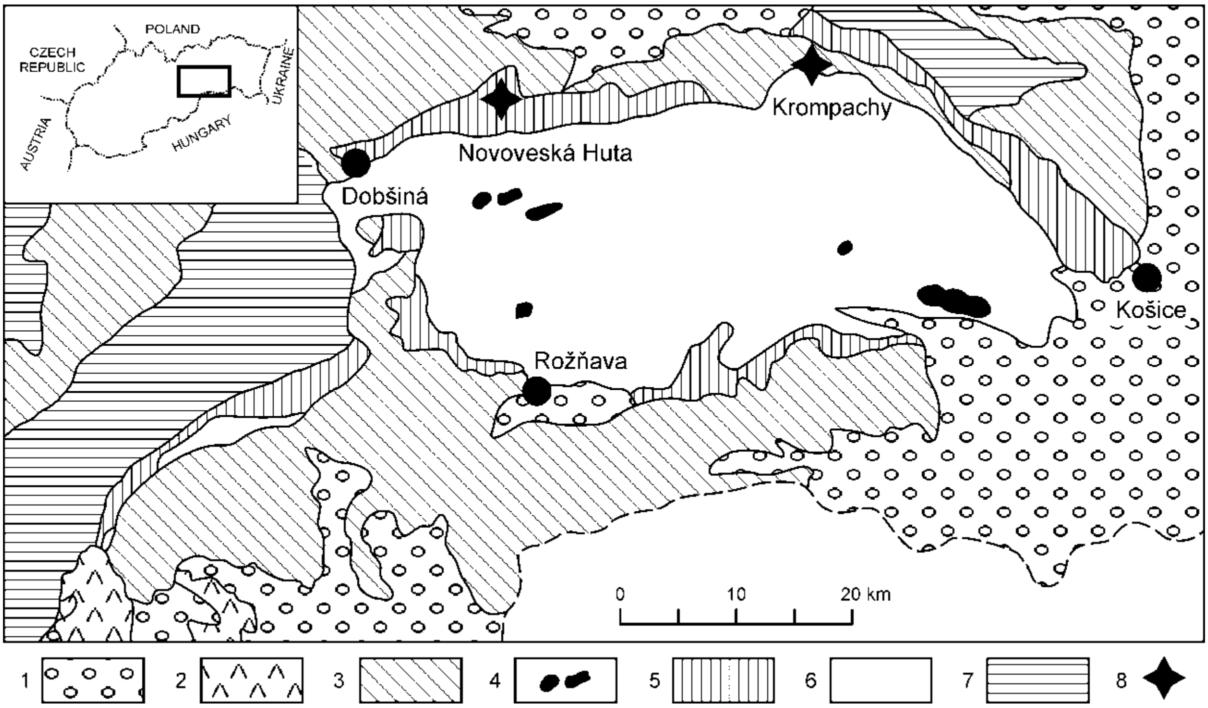

Fig. 1. Geological map of the eastern part of the Slovenské rudohorie Mts (adapted according to Biely et al. 1996). **1** — Tertiary sediments, **2** — Neogene volcanic rocks, **3** — Mesozoic rocks, **4–6** — Gemericum: 4 — granite, 5 — Upper Paleozoic rocks, 6 — Lower Paleozoic rocks, **7** — Paleozoic and Proterozoic? rocks of Veporicum, **8** — studied mineralization at **NH** — Novoveská Huta, **Kr** — Krompachy.

to -4.6 and from -6.3 to -2.5 ‰, respectively, in quartz-carbonate veins with copper mineralization suggest a deeper homogenized hydrothermal source of ore-bearing solutions (Rojkovič et al. 1993). The prevalence of uranogene Pb is typical for the stratiform U-Mo mineralization, whereas thorogene ^{208}Pb is characteristic of quartz-carbonate veins with copper mineralization (Zhukov & Rojkovič 1982).

Quartz-carbonate veins with copper mineralization were formed later. The veins cut older stratiform U-Mo mineralization. The older generation of the veins is represented in places by siderite-sulphide mineralization. The younger stage is represented by dominant Fe-dolomite and chalcopyrite. Copper mineralization in the studied rocks is represented by chalcopyrite and tennantite accompanied by carbonates (mostly Fe-dolomite), quartz, pyrite, galena, sphalerite, arsenopyrite, marcasite, boulangerite, clausthalite, cinnabar, barite and tourmaline. Younger uraninite occurs rarely. Quartz accompanying chalcopyrite displays homogenization temperatures of fluid inclusions from 150 to 230 °C with maximum 180 to 190 °C and corresponds to composition of $CaCl_2$-NaCl-H_2O and fluid concentration ranging from 20.6 to 22.6 equiv. wt. % NaCl. The less frequent solid phase is represented by carbonate. Quartz of the third stage of hydrothermal vein mineralization in Novoveská Huta gives T_{hom} from 120 to 190 °C, 7.1 equiv. wt. % NaCl and Fe-dolomite of the fifth stage gives T_{hom} from 95 to 130 °C and 17.2 equiv. wt. % NaCl (Rojkovič et al. 1993). Pb isotopic analysis in galena of quartz-carbonate veins with copper mineralization gave a model age of lead 110 Ma (Háber & Rojkovič 1989, according to Stacey & Kramers 1975).

Methods

Minerals were studied by polarizing microscope in both transmitted and in reflected light and by scanning electron microscope (SEM). They were analysed by wave-dispersion X-ray microanalysis (WDX) and by X-ray diffraction analysis (XRD). Microprobe analyses (WDX) were performed with CAMECA SX100 in the Department of Electron Microanalysis at Geological Survey of Slovak Republic in Bratislava under the following conditions: accelerating voltage 15 kV, beam current 20 nA and beam diameter of about 1-5 μm. The obtained counts were recalculated in oxides using the PAP correction. Natural and synthetic standards were applied on calibration of the microprobe: Al-Al_2O_3, Si-SiO_2, P-apatite, Ca-wollastonite, Y-YPO_4, La-$LaPO_4$, Ce-$CePO_4$, Gd-$GdPO_4$, Yb-$YbPO_4$, Sm-$SmPO_4$, Pr-$PrPO_4$, Er-$ErPO_4$, Nd-$NdPO_4$, Lu-$LuPO_4$, Ho-$HoPO_4$, Dy-$DyPO_4$, Tb-$TbPO_4$, Pb-PbS, U-UO_2 and Th-ThO_2.

Microprobe analyses of monazites were performed under different conditions. To obtain suitable counting statistics for measurement of low lead concentration as well as very precise measurement of U, Th and Y counting times 70-130 s and the beam current 100-130 nA were used. Measurement conditions and age calculations were described in more detail by Konečný et al. (2004). Th-U-Pb ages were recalculated after Montel et al. (1996) by MONDAT program (P. Konečný). The resulting age of each sample was calculated as the weighted average of individual ages, its errors are given on 95 % confidence level (2σ).

Table 1: Chemical composition of monazite in Novoveská Huta in weight %.

Sample	**NH-847/569.5**											
No	**1**	**2**	**3**	**4**	**5**	**6**	**7**	**8**	**9**	**10**	**11**	**12**
Y_2O_3	0.74	0.88	0.50	0.56	0.56	0.82	0.81	0.94	0.53	0.69	0.57	0.82
La_2O_3	16.87	15.54	17.24	16.81	16.83	16.06	16.22	16.07	17.51	16.86	17.71	16.43
Ce_2O_3	31.31	30.48	31.12	30.88	30.67	31.19	30.87	31.12	31.21	31.37	31.26	31.07
Pr_2O_3	3.08	3.33	3.15	3.11	3.02	3.14	3.19	3.33	3.22	3.09	3.13	3.29
Nd_2O_3	11.03	11.09	10.62	10.66	11.16	11.58	11.18	11.50	10.64	11.08	10.50	11.30
Sm_2O_3	1.33	1.43	1.14	1.32	1.22	1.45	1.60	1.31	1.18	1.24	1.16	1.49
Gd_2O_3	1.00	1.08	0.85	0.92	0.76	1.09	0.97	0.96	0.80	0.98	0.77	1.00
Tb_2O_3	0.00	0.07	0.00	0.08	0.05	0.08	0.00	0.04	0.00	0.08	0.01	0.13
Dy_2O_3	0.30	0.19	0.17	0.09	0.28	0.16	0.29	0.22	0.15	0.02	0.20	0.35
Ho_2O_3	0.29	0.23	0.44	0.49	0.02	0.62	0.49	0.23	0.18	0.64	0.43	0.29
Er_2O_3	0.00	0.00	0.10	0.00	0.05	0.13	0.00	0.16	0.00	0.02	0.06	0.00
Yb_2O_3	0.08	0.13	0.08	0.04	0.00	0.07	0.03	0.10	0.00	0.13	0.03	0.00
Lu_2O_3	0.00	0.17	0.04	0.00	0.00	0.00	0.00	0.00	0.00	0.00	0.00	0.00
PbO	0.07	0.08	0.08	0.08	0.08	0.06	0.06	0.06	0.08	0.07	0.08	0.07
UO_2	0.06	0.06	0.05	0.08	0.05	0.04	0.01	0.02	0.06	0.04	0.06	0.05
ThO_2	4.95	5.32	5.30	6.02	6.06	4.30	4.70	4.45	5.60	4.25	5.44	4.78
Al_2O_3	0.00	0.00	0.00	0.00	0.00	0.00	0.00	0.00	0.00	0.00	0.00	0.00
SiO_2	1.04	1.08	1.35	1.41	1.42	0.85	0.92	0.80	1.35	0.91	1.34	0.98
CaO	0.28	0.34	0.17	0.17	0.17	0.29	0.32	0.34	0.18	0.27	0.17	0.32
P_2O_5	27.44	27.25	26.90	26.98	26.78	27.76	27.35	27.82	26.66	27.76	27.11	26.95
Total	99.73	98.66	99.25	99.56	99.11	99.58	98.89	99.39	99.26	99.38	99.95	99.18
	Cations on the basis of 4 O											
Y	0.016	0.019	0.011	0.012	0.012	0.018	0.017	0.020	0.012	0.015	0.012	0.018
La	0.250	0.233	0.258	0.251	0.252	0.238	0.242	0.238	0.263	0.250	0.263	0.246
Ce	0.461	0.453	0.462	0.457	0.456	0.458	0.458	0.458	0.465	0.462	0.461	0.462
Pr	0.045	0.049	0.047	0.046	0.045	0.046	0.047	0.049	0.048	0.045	0.046	0.049
Nd	0.158	0.161	0.154	0.154	0.162	0.166	0.162	0.165	0.155	0.159	0.151	0.164
Sm	0.018	0.020	0.016	0.018	0.017	0.020	0.022	0.018	0.017	0.017	0.016	0.021
Gd	0.013	0.015	0.011	0.012	0.010	0.014	0.013	0.013	0.011	0.013	0.010	0.013
Tb	0.000	0.001	0.000	0.001	0.001	0.001	0.000	0.001	0.000	0.001	0.000	0.002
Dy	0.004	0.002	0.002	0.001	0.004	0.002	0.004	0.003	0.002	0.000	0.003	0.005
Ho	0.004	0.003	0.006	0.006	0.000	0.008	0.006	0.003	0.002	0.008	0.006	0.004
Er	0.000	0.000	0.001	0.000	0.001	0.002	0.000	0.002	0.000	0.000	0.001	0.000
Yb	0.001	0.002	0.001	0.000	0.000	0.001	0.000	0.001	0.000	0.002	0.000	0.000
Lu	0.000	0.002	0.001	0.000	0.000	0.000	0.000	0.000	0.000	0.000	0.000	0.000
Pb	0.001	0.001	0.001	0.001	0.001	0.001	0.001	0.001	0.001	0.001	0.001	0.001
U	0.000	0.001	0.000	0.001	0.000	0.000	0.000	0.000	0.001	0.000	0.001	0.000
Th	0.045	0.049	0.049	0.055	0.056	0.039	0.043	0.041	0.052	0.039	0.050	0.044
Al	0.000	0.000	0.000	0.000	0.000	0.000	0.000	0.000	0.000	0.000	0.000	0.000
Si	0.042	0.044	0.055	0.057	0.058	0.034	0.037	0.032	0.055	0.036	0.054	0.040
Ca	0.012	0.015	0.007	0.007	0.007	0.012	0.014	0.015	0.008	0.011	0.007	0.014
P	0.935	0.936	0.925	0.923	0.922	0.943	0.937	0.946	0.919	0.944	0.925	0.928
Total	2.025	2.024	2.024	2.022	2.022	2.024	2.027	2.023	2.026	2.022	2.023	2.032

Monazite occurrence

Monazite Ce[PO_4] was found in two rock samples. Psammitic rhyolite tuff which was taken from drilling core No. 847 of Uranium Survey in 569.5 m overlying rhyolite in 583 m. Three monazite grains (up to 50 mm in diameter) are enclosed in biotite (Fig. 2). Scanning electron microscopy in back-scattered electron image does not show any zonality or inherited cores. No alteration of monazite was observed. Monazite is accompanied in biotite by zircon and apatite. Chemical composition shows Th content up to 6 wt. % (Table 1).

In quartz veins near Krompachy monazite occurs in veinlets accompanied by xenotime-(Y) (Fig. 3). Monazite aggregate 120×20 μm with homogeneous grains (up to 20 μm) without zonality (Fig. 4) was analysed. Chemical composition shows ThO_2 content up to 8 wt. % (Table 2). Analysed grains from both occurrences correspond to monazite (Fig. 5). Monazite from Novoveská Huta is closely bound

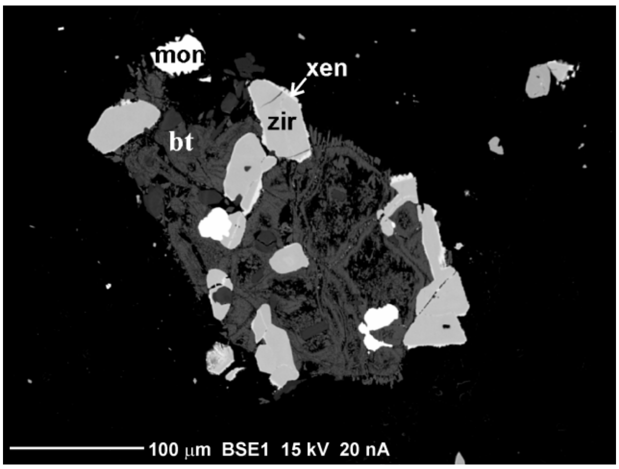

Fig. 2. Analysed monazite grains (**mon**), zircon (**zir**) with thin xenotime rim (**xen**) and biotite (**bt**) in rhyolite tuff, Novoveská Huta, SEM-BEI.

Table 2: Chemical composition of monazite in Krompachy in weight %.

Sample	Kr 6							
No	13	14	15	16	17	18	19	20
Y_2O_3	0.31	0.44	0.50	0.22	0.26	0.51	0.36	0.71
La_2O_3	3.40	3.00	3.08	3.70	3.69	2.46	3.05	2.70
Ce_2O_3	27.31	26.27	26.21	28.03	27.87	24.02	26.79	24.17
Pr_2O_3	4.49	4.60	4.65	4.47	4.26	4.61	5.13	4.90
Nd_2O_3	19.06	20.85	20.80	18.20	18.42	22.30	22.67	21.81
Sm_2O_3	4.55	5.16	5.10	3.84	3.99	6.17	5.41	6.35
Gd_2O_3	2.37	3.02	3.12	2.09	2.24	3.66	3.08	4.05
Tb_2O_3	0.03	0.01	0.07	0.03	0.08	0.10	0.00	0.19
Dy_2O_3	0.28	0.55	0.45	0.14	0.34	0.68	0.31	0.53
Ho_2O_3	0.65	0.00	0.30	0.16	0.39	0.01	0.26	0.03
Er_2O_3	0.04	0.16	0.07	0.02	0.17	0.16	0.00	0.00
Yb_2O_3	0.09	0.01	0.10	0.00	0.03	0.19	0.12	0.00
Lu_2O_3	0.00	0.00	0.00	0.00	0.00	0.00	0.00	0.00
PbO	0.05	0.03	0.05	0.04	0.06	0.03	0.03	0.03
UO_2	0.08	0.09	0.25	0.11	0.16	0.13	0.09	0.31
ThO_2	6.96	4.82	4.61	7.85	7.92	4.81	2.88	4.27
Al_2O_3	0.00	0.00	0.00	0.00	0.00	0.00	0.00	0.00
SiO_2	0.34	0.22	0.22	0.44	0.43	0.22	0.23	0.19
CaO	1.02	0.73	0.70	1.15	1.18	0.87	0.56	0.78
P_2O_5	27.88	28.71	28.45	27.85	28.10	28.52	28.36	28.91
Total	98.64	98.33	98.43	98.12	99.35	99.11	98.98	99.59
	Cations on the basis of 4 O							
Y	0.007	0.009	0.011	0.005	0.006	0.011	0.008	0.015
La	0.050	0.044	0.045	0.055	0.054	0.036	0.045	0.039
Ce	0.402	0.382	0.383	0.414	0.408	0.348	0.390	0.346
Pr	0.066	0.067	0.068	0.066	0.062	0.066	0.074	0.070
Nd	0.274	0.296	0.296	0.262	0.263	0.315	0.322	0.305
Sm	0.063	0.071	0.070	0.054	0.055	0.084	0.074	0.086
Gd	0.032	0.040	0.041	0.028	0.030	0.048	0.041	0.053
Tb	0.000	0.000	0.001	0.000	0.001	0.001	0.000	0.002
Dy	0.004	0.007	0.006	0.002	0.004	0.009	0.004	0.007
Ho	0.008	0.000	0.004	0.002	0.005	0.000	0.003	0.000
Er	0.000	0.002	0.001	0.000	0.002	0.002	0.000	0.000
Yb	0.001	0.000	0.001	0.000	0.000	0.002	0.001	0.000
Lu	0.000	0.000	0.000	0.000	0.000	0.000	0.000	0.000
Pb	0.001	0.000	0.000	0.000	0.001	0.000	0.000	0.000
U	0.001	0.001	0.002	0.001	0.001	0.001	0.001	0.003
Th	0.064	0.044	0.042	0.072	0.072	0.043	0.026	0.038
Al	0.000	0.000	0.000	0.000	0.000	0.000	0.000	0.000
Si	0.013	0.009	0.009	0.018	0.017	0.009	0.009	0.007
Ca	0.044	0.031	0.030	0.050	0.051	0.037	0.024	0.033
P	0.949	0.966	0.960	0.952	0.950	0.955	0.954	0.958
Total	2.044	2.039	2.042	2.036	2.038	2.053	2.051	2.051

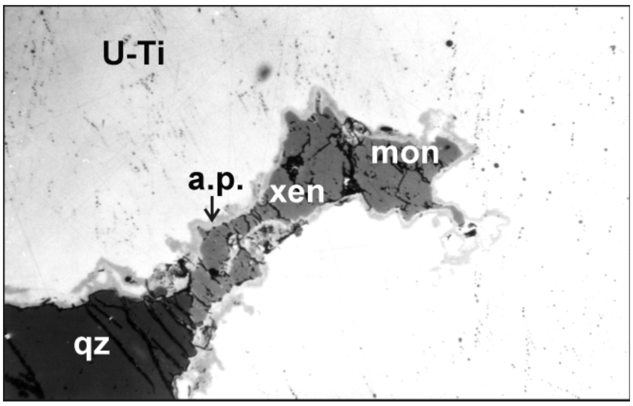

Fig. 3. Aggregate of U-Ti oxide (**U-Ti**) is cut by quartz veinlet (**qz**) with monazite (**mon**) and xenotime (**xen**). Veinlet is rimmed by alteration products of U-Ti oxide (a.p.) represented by Ti-oxide, Fe-hydroxide and secondary uranium minerals. Reflected light, parallel nicols.

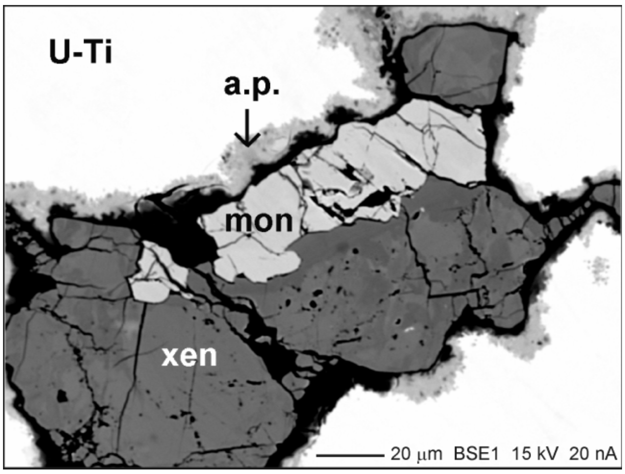

Fig. 4. U-Ti oxide (**U-Ti**) with veinlet of xenotime (**xen**) and analysed monazite (**mon**) rimmed by alteration products of U-Ti oxide (**a.p.**). SEM–BEI.

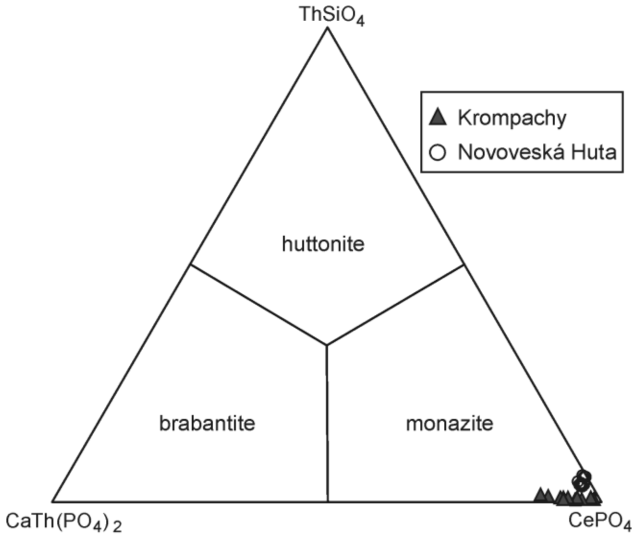

Fig. 5. Diagram of monazite composition from Novoveská Huta and Krompachy.

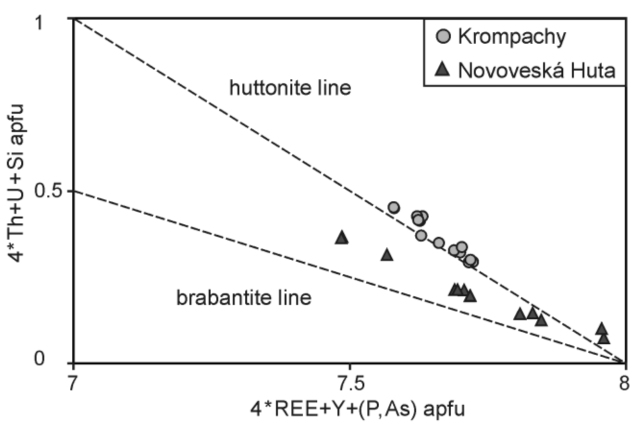

Fig. 6. (REE + Y + P) vs. (Th + U + Si) plot of analysed monazite.

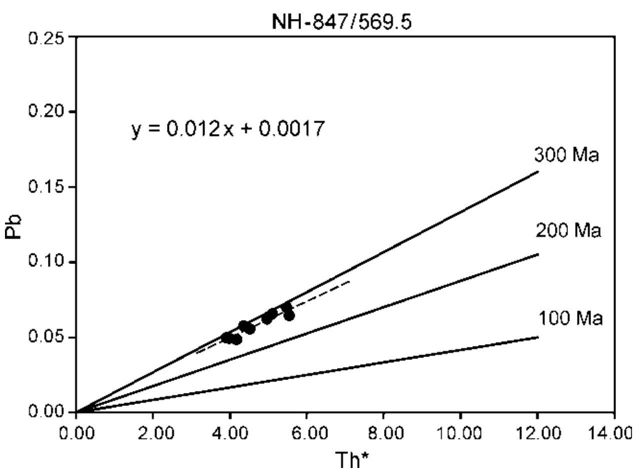

Fig. 7. Pb vs. Th* plots of monazite in rhyolite metatuff with isochrons from 100 to 300 Ma and with regression line fitted by least squares method. Near zero intersection of isochron is indicated by equation. Th* includes measured Th plus Th equivalent of measured U according to equation Th* = Th + 3.15 U (Nagy et al. 2002).

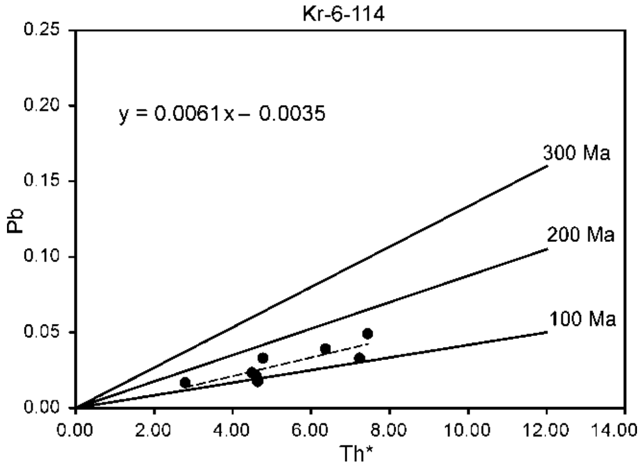

Fig. 8. Pb vs. Th* plots with isochrons and regression line as in Fig. 7 of monazite in quartz vein with uranium mineralization.

to the huttonite line, while monazite from Krompachy is slightly shifted towards the brabantite line (Fig. 6). Th-U-Pb dating of monazite from Novoveská Huta gave 278±10.2 Ma (Table 3, Fig. 7) and Th-U-Pb dating of vein monazite associated with uranium mineralization in Krompachy gave 124±10.2 Ma (Table 3, Fig. 8).

Associated minerals

Several phases associated with monazite were distinguished by polarizing microscope, scanning electron microscope, wave-dispersion X-ray microanalysis and by X-ray diffraction.

U-Ti oxides

Relatively homogeneous aggregates in polarizing and electron microscope. They are distinctly darker in reflected light than enclosed rutile. They are dominant in the Krompachy locality, where aggregates up to 2 cm were found. It is accompanied by quartz gangue and encloses columnar rutile and galena. It is cut by veinlets of younger quartz accompanied by xenotime-(Y) and monazite-(Ce). Xenomorphic U-Ti oxide is close to the chemical composition of UTi_2O_6 — brannerite (Table 4). X-ray diffraction of UTi_2O_6 from Krompachy as well as electron X-ray diffraction from Novoveská Huta confirmed the amorphousness of the material. This is not a proof of metamictization process, but it also excludes a presence of polymineral crystalline aggregate of rutile (or other Ti-oxide) and uraninite. U-Ti oxides are replaced by fine-grained often zoned alteration products represented by Ti-oxides, iron hydroxides and secondary uranium minerals.

Rutile TiO_2 is grey with a brownish tint and abundant yellowish brown internal reflection in reflected light. Rutile exhibits bireflection and strong anisotropy (light grey-dark violet brown). Rutile forms elongated grains (from 10 to 50 μm long), columns (from 0.02 to 0.2 mm long) and irregu-

Table 3: Monazite dating. Th, U, Pb and Y concentrations in monazite in weight %. Ages (T) calculated after model of Montel et al. (1996). **NH** — Novoveská Huta, **Kr** — Krompachy.

Sample	No	Th	U	Pb	$2\sigma_{Pb}$ (wt. %)	Y	T (Ma)	$2\sigma_T$ (Ma)
NH-847/569.5	1	4.3490	0.0811	0.0703	0.0071	0.5822	275	± 35.2
NH-847/569.5 v	2	4.6757	0.0835	0.0858	0.0071	0.6936	321	± 32.3
NH-847/569.5 v	3	4.6542	0.0786	0.0815	0.0071	0.3937	322	± 32.8
NH-847/569.5	4	5.2879	0.1115	0.0774	0.0071	0.4423	261	± 28.6
NH-847/569.5	5	5.3285	0.0803	0.0826	0.0071	0.4397	285	± 29.1
NH-847/569.5	6	3.7779	0.0663	0.0651	0.0071	0.6487	283	± 40.3
NH-847/569.5	7	4.1341	0.0388	0.0640	0.0071	0.6395	260	± 38.0
NH-847/569.5	8	3.9130	0.0461	0.0659	0.0071	0.7395	276	± 39.4
NH-847/569.5	9	4.9228	0.0873	0.0783	0.0072	0.4207	288	± 30.9
NH-847/569.5 v	10	3.7374	0.0585	0.0700	0.0070	0.5403	324	± 40.8
NH-847/569.5	11	4.7835	0.0866	0.0752	0.0072	0.4519	280	± 31.9
NH-847/569.5	12	4.2024	0.0751	0.0730	0.0071	0.6459	295	± 36.1
Kr-6-114	13	6.1185	0.1131	0.0495	0.0071	0.2445	138	± 25.1
Kr-6-114	14	4.2315	0.1084	0.0351	0.0070	0.3435	117	± 35.2
Kr-6-114	15	4.0534	0.2493	0.0451	0.0070	0.3895	155	± 32.8
Kr-6-114	16	6.8973	0.1477	0.0424	0.0071	0.1711	102	± 22.0
Kr-6-114	17	6.9639	0.1904	0.0590	0.0072	0.2062	148	± 21.8
Kr-6-114	18	4.2225	0.1446	0.0331	0.0070	0.4009	101	± 34.2
Kr-6-114	19	2.5322	0.0942	0.0276	0.0070	0.2826	135	± 56.0
Kr-6-114	20	3.7482	0.3019	0.0318	0.0070	0.5587	85	± 34.0
					Resulting age			
NH-847/569					278±11.2 Ma			
Kr-6					124±10.2 Ma			

lar grains (mostly from 5 to 50 μm in size). WDX and EDX analyses show a homogeneous distribution of iron and also increased contents of niobium in rutile from Krompachy (Table 5).

Table 4: Chemical composition of U-Ti oxides in Krompachy in weight %.

Sample No	Kr6b 1	Kr6b 2	Kr12a 3	Kr12b 4
SiO_2	0.97	0.79	0.86	0.85
TiO_2	34.84	33.97	33.91	33.96
ThO_2	4.42	6.64	4.30	3.69
UO_2	49.91	49.68	50.44	51.29
Fe_2O_3	1.14	1.64	2.34	1.59
Y_2O_3	0.57	0.17	0.25	0.43
Nb_2O_3	0.04	0.00	0.01	0.33
La_2O_3	0.00	0.00	0.00	0.00
Ce_2O_3	0.00	0.00	0.00	0.00
Nd_2O_3	0.41	0.00	0.00	0.00
CaO	1.67	1.67	1.67	1.68
PbO	0.88	0.56	0.53	0.64
Total	94.85	95.12	94.31	94.46
	Cations on the basis of 6 O			
Si	0.071	0.058	0.063	0.063
Ti	1.904	1.875	1.868	1.877
Th	0.073	0.111	0.072	0.062
U	0.807	0.812	0.822	0.839
Fe	0.062	0.091	0.129	0.088
Y	0.022	0.007	0.010	0.017
Nb	0.002	0.000	0.000	0.013
La	0.000	0.000	0.000	0.000
Ce	0.000	0.000	0.000	0.000
Nd	0.011	0.000	0.000	0.000
Ca	0.130	0.131	0.131	0.132
Pb	0.017	0.011	0.011	0.013
Total	3.098	3.096	3.106	3.102

Xenotime $Y[PO_4]$ occurs in quartz veinlets around 0.1 mm thick cutting homogeneous U-Ti oxide (Fig. 4). Xenotime forms thin rims around accessory zircon in the Permian rhyolite tuff in Novoveská Huta (Fig. 2). Clusters and veinlets of xenotime-(Y) are abundant in other occurrences of the mineralized Permian rocks.

Heavy rare earth elements (HREE) from Gd to Yb are also present in the xenotime besides the dominant Y and P due to their close ionic radii to Y (Table 6). It contains higher uranium and lower thorium contents compared to monazite. Zonality of xenotime-(Y) reflects variability of radioactive elements and rare earth elements contents.

Galena PbS forms admixtures up to 0.05 mm in size enclosed in U-Ti oxides. Its identification was confirmed by WDS chemical composition corresponding to $Pb_{0.99}S_{1.01}$.

Table 5: Chemical composition of rutile in Krompachy in weight %.

Sample No	Kr6b 1	Kr12b 2	Kr12b 3	Kr6a 4
TiO_2	93.85	90.65	89.86	89.57
ThO_2	0.00	0.00	0.02	0.00
UO_2	0.00	0.04	0.01	0.14
Fe_2O_3	2.27	2.27	2.75	3.10
Nb_2O_3	1.86	4.62	5.05	4.86
Total	97.98	97.58	97.69	97.67
	Cations on the basis of 2 O			
Ti	0.973	0.957	0.951	0.949
Th	0.000	0.000	0.000	0.000
U	0.000	0.000	0.000	0.000
Fe	0.024	0.024	0.029	0.033
Nb	0.013	0.033	0.037	0.035
Total	1.009	1.014	1.016	1.017

Table 6: Chemical composition of xenotime in Krompachy in weight %.

Sample				**Kr 6**			
No	**1**	**2**	**3**	**4**	**5**	**6**	**7**
Y_2O_3	36.59	35.78	36.38	37.81	39.00	38.70	36.47
Ce_2O_3	0.07	0.00	0.00	0.00	0.00	0.18	0.01
Nd_2O_3	0.48	0.63	0.15	0.12	0.17	0.32	0.62
Sm_2O_3	1.89	1.86	1.39	1.07	0.57	0.81	1.67
Eu_2O_3	2.34	2.10	2.41	1.92	1.87	2.16	2.42
Gd_2O_3	6.74	7.27	6.04	5.63	6.29	5.83	6.84
Tb2O3	1.32	1.55	1.00	1.09	1.16	1.22	1.35
Dy_2O_3	8.67	8.41	8.11	7.79	8.25	7.67	9.01
Ho_2O_3	0.93	1.28	1.64	1.46	1.36	1.08	1.23
Er_2O_3	3.59	3.89	4.28	4.25	3.42	3.93	3.33
Tm_2O_3	0.62	0.63	0.59	0.79	0.49	0.56	0.70
Yb_2O_3	2.67	2.36	2.56	3.01	2.06	2.55	2.25
Lu_2O_3	0.56	0.71	0.37	0.83	0.51	1.21	0.31
ThO_2	0.42	0.39	1.44	1.31	0.25	0.61	0.08
UO_2	0.19	0.24	0.86	0.91	0.26	0.55	0.12
F	0.48	0.34	0.00	0.20	0.24	0.50	1.06
P_2O_5	33.86	33.46	33.26	32.94	34.12	33.88	33.34
Total	101.42	100.90	100.48	101.13	100.02	101.76	100.81
				Cations on the basis of 4 O			
Y	0.676	0.667	0.680	0.705	0.716	0.710	0.682
Ce	0.001	0.000	0.000	0.000	0.000	0.002	0.000
Nd	0.006	0.008	0.002	0.002	0.002	0.004	0.008
Sm	0.023	0.022	0.017	0.013	0.007	0.010	0.020
Eu	0.028	0.025	0.029	0.023	0.022	0.025	0.029
Gd	0.078	0.084	0.070	0.065	0.072	0.067	0.080
Tb	0.015	0.018	0.012	0.013	0.013	0.014	0.016
Dy	0.097	0.095	0.092	0.088	0.092	0.085	0.102
Ho	0.010	0.014	0.018	0.016	0.015	0.012	0.014
Er	0.039	0.043	0.047	0.047	0.037	0.043	0.037
Tm	0.007	0.007	0.007	0.009	0.005	0.006	0.008
Yb	0.028	0.025	0.027	0.032	0.022	0.027	0.024
Lu	0.006	0.008	0.004	0.009	0.005	0.013	0.003
Th	0.003	0.003	0.012	0.011	0.002	0.005	0.001
U	0.002	0.002	0.007	0.007	0.002	0.004	0.001
F	0.053	0.038	0.000	0.022	0.026	0.055	0.118
P	0.994	0.992	0.989	0.978	0.997	0.988	0.992
Total	2.064	2.050	2.011	2.039	2.035	2.068	2.133

Quartz and albite (Table 7) represent dominant gangue minerals.

Discussion

Uranium mineralization in the Permian sequences of the Gemericum of the Western Carpathians is related to the Permian acid volcanic and volcanoclastic rocks. Acid volcanites and their tuffs are the potential “protoliths” of U, Mo, Cu and associated elements accumulations. The new results of Th-U-Pb dating of monazite confirm the age of monazite in the Permian tuff of rhyolite from Novoveská Huta (drilling hole 847, 569.5 m) 278 ± 11.2 Ma. U-Pb dating of zircons in metarhyodacite from Čierny Balog and Bacúch (Slovakia) shows ages of 278 ± 11 and 255 ± 2 Ma (Kotov et al. 1996). The Permian age of zircon 284 ± 3 Ma is also known from metavolcanics of “Porphyrmaterialschiefer” from the Tauernfenster in Austria (Söllner et al. 1991).

A substantial part of uranium in the non-mineralized volcanic rocks and their tuffs is bound to the matrix, but its distribution is irregular. Irregular distribution is documented by histograms of uranium content and by fission tracks (Rojkovič et al. 1991). Low-grade ores were formed during diagenesis after uranium release from devitrificated tuffs and tuffitic rocks. Stratiform mineralization started during the Upper Permian shortly after deposition and burial by overlying sediments within aquiferous horizons of permeable rocks. Ground water in oxidic and acid conditions took part in leaching and transport of U. Accumulations of pyrite, uraninite, Mo and Cu sulphides were formed, due to mixing of oxidative meteoric solutions with solutions derived from reducing hot springs (H_2S), and partly with organic matter. U-Pb isotopic dating of the low-grade stratiform uranium mineralization gave 240 ± 30 Ma in Novoveská Huta (Arapov et al. 1984). Similar ages of uranium mineralization were found in the Permian rocks of the Alps. Uranium mineralization near Val Vedello in Italy gives from 249 to 240 Ma (Cadel et al. 1987). U-Pb discordia dating of uranium mineralization from Valais in Switzerland indicates the primary age of crystallization around 255 Ma (Eikenberg et al. 1989).

Table 7: Chemical composition of albite in Krompachy in weight %.

Sample	Kr 12a		
No	1	2	3
SiO_2	68.66	68.64	68.10
Al_2O_3	19.63	19.23	19.63
MgO	0.00	0.01	0.00
CaO	0.02	0.04	0.36
FeO	0.07	0.06	0.01
BaO	0.00	0.00	0.00
Na_2O	11.85	11.68	11.46
K_2O	0.05	0.05	0.07
Total	100.28	99.71	99.63
	Cations on the basis of 8 O		
Si	2.991	3.005	2.986
Al	1.008	0.992	1.014
Mg	0.000	0.001	0.000
Ca	0.001	0.002	0.017
Fe	0.003	0.002	0.000
Ba	0.000	0.000	0.000
Na	1.001	0.991	0.974
K	0.003	0.003	0.004
Total	5.007	4.996	4.996

The Alpine tectono-metamorphic processes created structures in which hydrothermal fluids could circulate. U-Mo mineralization from low-grade stratiform mineralization was remobilized and concentrated (Rojkovič 1997). Sericitization, silicification and deposition of apatite preceded the remobilization. Characteristic for this process are veinlets and disseminated uraninite, coffinite and U-Ti oxides including brannerite. They are accompanied by pyrite, molybdenite, chalcopyrite, galena, pyrrhotite, montroseite, xenotime-(Y), monazite-(Ce) and quartz. This mineralization is close by age and composition to remobilized stratiform U-Mo mineralization in volcanoclastic and volcanic rocks mentioned before. Remobilized U-Mo mineralization was formed at temperatures ranging from 320 to 240 °C with maximum at 250 °C (Rojkovič et al. 1993). Hydrothermal solutions have mobilized during compression associated with continental collision similarly as Early to middle Cretaceous quartz-ankerite-sulphidic veins (Hurai et al. 2002). According to the U-Pb dating, the age of high-grade uranium ore near faults gave the Alpine age of 130±20 Ma (Arapov et al. 1984). The Cretaceous age of uranium ore remobilization in the Permian rocks (from 80 to 110 Ma) is known from several deposits (Mittempergher 1972; Petrascheck et al. 1977; Lancelot et al. 1984). The results of Th-U-Pb dating of vein monazite from Krompachy associated with uranium mineralization confirm the age of 124±10.2 Ma.

Recent results of Th-U-Pb dating of monazite confirm the Permian age of acid volcanism and the Cretaceous age of remobilized vein uranium mineralization.

Acknowledgments: The study was supported by Project 503 at the Ministry of the Environment and Grant VEGA 1/1026/04. The development of monazite dating method was supported by Project 12-01-9/100 at the Ministry of the Environment, SR. This manuscript benefited greatly from the reviews of I. Petrík, M. Svojtka and G. Nagy.

References

Arapov J.A., Bojcov V.J., Česnokov N.I., Djakonov A.V., Halbrštát J., Jakovjenko A.M., Kolek M., Komínek J., Kozyrev V.N., Kremčukov G.A., Lažanský M., Milovanov I.A., Nový V. & Šorf F. (Eds.) 1984: Czechoslovak uranium deposits. *SNTL,* Praha, 1–365 (in Czech).

Bajaník Š., Vozárová A. & Reichwalder P. 1981: Litostratigraphic classification of the Rakovec Group and the Late Paleozoic in the Spišsko-gemerské Rudohorie Mts. *Geol. Práce, Spr.* 75, 27–56 (in Slovak).

Biely A., Bezák V., Elečko M., Kaličiak M., Konečný V., Lexa J., Mello J., Nemčok J., Potfaj M., Rakús M., Vass D., Vozár J. & Vozárová A. 1996: Geological map of Slovakia. 1:500,000. *Geol. Surv. Slovak Republic,* Bratislava.

Cadel G., Meneghel L. & Fuchs Y. 1987: Uranium mineralization associated with the evolution of a Permo-Carboniferous volcanic field: examples from Novazza and Val Vedello (Northern Italy). *Uranium* 3, 407–421.

Cocherie A. & Albarede F. 2001: An improved U-Th-Pb age calculation for electron microprobe dating of monazite. *Geochim. Cosmochim. Acta* 65, 24, 4509–4522.

Cocherie A., Legendre O., Peucat J.J. & Kouamelan A.N. 1998: Geochronology of polygenetic monazites constrained by in situ electron microprobe Th-U-total lead determination: Implications for lead behaviour in monazite. *Geochim. Cosmochim. Acta* 62, 2475–2497.

Eikenberg J., Köppel V., Labhart T. & Signer P. 1989: U-Pb, U-Xe and U-Kr systematics of a greenschist facies metamorphic uranium mineralization of the Siviez-Mischabel nappe (Valais, Switzerland). *Schweiz. Mineral. Petrogr. Mitt.* 69, 331–344.

Faryad S.W. & Dianiška I. 1999: Alpine overprint in the Early Paleozoic of the Gemericum. *Miner. Slovaca* 31, 485–490 (in Slovak).

Fialin M., Rémy H., Richard C. & Wagner Ch. 1999: Trace element analysis with electron microprobe: New data and perspectives. *Amer. Mineralogist* 84, 70–77.

Finger F. & Broska I. 1999: The Gemeric S-type granites in southeastern Slovakia: late Palaeozoic or Alpine intrusion? Evidence from electron-microprobe dating of monazite. *Schweiz. Mineral. Petrogr. Mitt.* 79, 439–443.

Finger F., Broska I., Haunschmid B., Hraško Ľ., Kohút M., Krenn E., Petrík I., Riegler G. & Uher P. 2003: Electron-microprobe dating of monazites from Western Carpathian basement granitoids: plutonic evidence for an important Permian rifting event subsequent to Variscan crustal anatexis. *Int. J. Earth Sci.* 92, 86–98.

Háber M. & Rojkovič I. 1989: Metallogeny of the Permian of the Slovenské rudohorie Mts., Czechoslovakia. In: *XIVth Congress of Carpatho-Balkan Geological Association,* Sofia, 1355–1358.

Hurai V., Harčová E., Huraiová M., Ozdín D., Prochaska W. & Wiegerová V. 2002: Origin of siderite veins in the Western Carpathians I. P-T-X-δ^{13} C-δ^{18}O relations in ore-forming brines of the Rudňany deposits. *Ore Geol. Rev.* 21, 67–101.

Kohn M.J. & Malloy M.A. 2004: Formation of monazite via prograde metamorhhic reactions among common silicates: Implications for age determinations. *Geochim. Cosmochim. Acta* 68, 1, 101–113.

Konečný P., Siman P., Holický I., Janák M. & Kollárová V. 2004: Method of monazite dating by means of the electron microprobe. *Miner. Slovaca* 36, 225–235 (in Slovak).

Kotov A.B., Miko O., Putiš M., Korikovsky S.P., Salnikova E.B., Kovach V.P., Yakovleva S.Z., Bereznaya N.G., Kráľ J. & Krist E. 1996: U/Pb dating of zircons of postorogenic acid metavolcanics: a record of Permian-Triassic taphrogeny of the West-Carpathian basement. *Geol. Carpathica* 47, 73–79.

Lancelot J.R., Saint André B. & Boisse H. 1984: Systematique U-Pb et evolution du gisement d'uranium de Lodéve (France). *Mineral. Deposita* 19, 44–53.

Mittempergher M. 1972: The paleogeographical, lithological and structural controls of uranium occurrences in the Alps. In: *2nd International symposium on the mineral deposits of the Alps,* Ljubljana, 63–76.

Montel J.M., Foret S., Veschambre M., Nicollet Ch. & Provost A. 1996: Electron microprobe dating of monazite. *Chem. Geol.* 131, 37–53.

Nagy G. 2003: Problems of monazite dating by EPMA. *Acta Mineral. Petrogr. Szeged* 1, 76.

Nagy G., Draganits E., Demény A., Pantó G. & Árkai P. 2002: Genesis and transformations of monazite, florencite and rhabdophane during medium grade metamorphism: examples from the Sopron Hills, Eastern Alps. *Chem. Geol.* 191, 25–46.

Novotný L. & Miháľ F. 1987: New lithostratigraphic units in the Krompachy Group. *Miner. Slovaca* 19, 97–113 (in Slovak).

Parrish R.R. 1990: U-Pb dating of monazite and its application to geological problems. *Canad. J. Earth Sci.* 27, 1431–1450.

Petrascheck W.E., Erkan E. & Siegl W. 1977: Type of uranium deposits in the Austrian Alps. In: Geology, mining and extractive processing of uranium. *IMM,* London, 71–75.

Plašienka D., Grecula P., Putiš M., Kováč M. & Hovorka D. 1997: Evolution and structure of the Western Carpathians: an overview. In: Grecula P., Hovorka D. & Putiš M. (Eds.): Geological evolution of the Western Carpathians. *Miner. Slovaca — Monograph,* Bratislava, 1–24.

Pyle J.M., Spear F.S. & Wark D. 2002: Electron microprobe analysis of REE in apatite, monazite and xenotime: protocols and pitfalls. *Rew. Mineral. Geochem.* 48, 337–362.

Rojkovič I. 1968: Mineralogical-geochemical characterization of U-Mo-Cu mineralization in the Permian of the Spišsko-gemerské rudohorie Mts. *Geol. Zbor. Geol. Carpath.* 19, 179–204.

Rojkovič I. 1997: Uranium mineralization in Slovakia. *Acta Geol. Univ. Comen., Monographic Ser.* 1–117.

Rojkovič I. & Miháľ F. 1991: Geological structure and uranium mineralization in the Permian rocks of the north-eastern part of the Slovenské Rudohorie Mts. *Miner. Slovaca* 23, 123–132 (in Slovak).

Rojkovič I., Kráľ J., Kátlovský V. & Pavlovič J. 1991: Uranium distribution in volcanic and volcanoclastic rocks of the northern Gemeric Permian. *Geol. Carpathica* 42, 105–110.

Rojkovič I., Novotný L. & Háber M. 1993: Stratiform and vein U, Mo and Cu mineralization in the Novoveská Huta area, ČSFR. *Mineral. Deposita* 28, 58–65.

Scherer M., Engi M., Gnos E., Jakob V. & Liechti A. 2000: Monazite analysis; from sample preparation to microprobe age dating and REE quantification. *Schweiz. Mineral. Petrogr. Mitt.* 80, 93–105.

Söllner F., Höll R. & Miller H. 1991: U-Pb-Systematik der Zirkone in meta-Vulkaniten ("Porphyroiden") aus der Nördlichen Grauwackenzone und dem Tauernfenster (Ostalpen, Österreich). *Z. Dtsch. Geol. Gesell.* 142, 285–299.

Stacey J.S. & Kramers J.D. 1975: Approximation of terrestrial lead isotope evolution by a two-stage model. *Earth Planet. Sci. Lett.* 26, 207–221.

Suzuki K. & Adachi M. 1991: The chemical Th-U-total Pb isochron ages of zircon and monazite from the Gray Granite of the Hida Terrane, Japan. *J. Earth Sci., Nagoya Univ.* 38, 11–37.

Suzuki K. & Adachi M. 1994: Middle Precambrian detrital monazite and zircon from Hida gneiss on Oki-Dogo Island, Japan: their origin and implications for correlation of basement gneiss of Southwest Japan and Korea. *Tectonophysics* 235, 277–292.

Suzuki K. & Adachi M. 1998: Denudation history of the high T/P Ryoky metamorphic belt, southwest Japan: constraints from CHIME monazite ages of gneisses and granitoids. *J. Metamorphic Geology* 16, 23–37.

Suzuki K., Adachi M. & Kajizuka I. 1994: Electron microprobe observations of Pb diffusion in metamorphosed detrital monazites. *Earth Planet. Sci. Lett.* 128, 391–405.

Vozárová A. & Vozár J. 1988: Late Paleozoic in West Carpathians. *Veda,* Bratislava, 1–314.

Williams M.L., Jercinovic M.J. & Terry M.P. 1999. Age mapping and dating of monazite on the electron microprobe: Deconvoluting multistage tectonic histories. *Geology* 27, 1023–1026.

Zhukov F.I. & Rojkovič I. 1982: Isotopic composition of sulphur and carbon of uranium mineralization near Novoveská Huta (Slovenské rudohorie Mts.). In: *Symposium on geochemistry of endogenous and exogenous processes,* Bratislava, 241–255.